Assessment of Empirical Near-Shore Bathymetry Model Using New Emerged PlanetScope Instrument and Sentinel-2 Data in Coastal Shallow Waters

Khakhim, N.,[1*] Kurniawan, A.,[2] Wicaksono., P.[1] and Hasrul A.[2]
[1]Department of Geography Information Science, Faculty of Geography, Universitas Gadjah Mada, Indonesia
E-mail: nurulk@ugm.ac.id,* prama.wicaksono@ugm.ac.id
[2]Coastal and Watershed Management Planning, Postgraduate Geography, Universitas Gadjah Mada, Indonesia, E-mail: agung.kurniawan.16@mail.ugm.ac.id, ahmad.hasrul@mail.ugm.ac.id
Corresponding Author

DOI: https://doi.org/10.52939/ijg.v20i2.3071

Abstract
Shallow water bathymetric information is important for human life because it has a strong influence on phenomena and dynamics in coastal areas. Conventional bathymetric mapping methods are capable of obtaining high-precision accuracy, but require expensive and complex resources. Specifically, in shallow waters, survey instruments have difficulty obtaining adequate depth data due to the many obstacles that must be overcome. Remote sensing-based shallow water bathymetry called as Satellite-Derived Bathymetry (SDB) is a reasonable and efficient choice. Technological developments enable SDB data processing to be much more efficient in terms of time and storage by utilizing cloud-based platforms such as Google Earth Engine (GEE). Spatial and temporal resolution is still a challenge in SDB, so in this condition PlanetScope with daily temporal resolution capabilities is an optimistic choice. However, this image falls into a relatively new image category. In this study we tested the performance of Sentinel-2A imagery and new PlanetScope imagery bands. The existence of the new sensor owned by PlanetScope allows an increased choice of SDB data sources with high spatial and temporal resolution that is better than the general datasets currently available. There are four additional channels are Coastal Blue, Green I, Yellow, and Red Edge. Assessment is needed to test the capabilities of each new channel using empirical methods via the Stumpf algorithm. Based on accuracy assessment observations, the Sentinel-2A channel combination is still better in terms of accuracy and determination, because it is able to represent the depth in the study area up to 70%. The potential use of PlanetScope's new channels for SDB applications can still be seen in the combination of the Coastal Blue and Yellow channels. This channel combination is still able to represent 47% of the depth variations in the study area.

Keywords: Cloud computing, Google earth engine, PlanetScope, Satellite-Derived Bathymetry, Shallow water, Stumpf Algorithm, Sentinel-2A

1. Introduction

Understanding and mapping the surface of planet Earth requires the help of remote sensing as an "eye" that moves in space. Related themes in tropical areas and their influence on communities have been widely discussed using geographic data obtained through remote sensing [1]. 2016 was the era when the PlanetScope satellite was officially launched for the first time [2] and until now it has been widely used for various applications to monitor the earth's surface, such as land cover mapping efficiency [3], hydrological connectivity phenomena [4] and coastal areas [5]. In the coastal sector, several studies have been carried out to test the ability of PlanetScope satellite imagery to obtain shallow water depth information, both empirically [6] and analytically [7]. However, technological developments have brought more advanced approaches based on machine learning [8] and [9] to deep learning [10] and [11]. Shallow water bathymetric information is a crucial component [9] for establishing marine conservation areas [12] and [13], input in the preparation of marine navigation maps [14], and plays an important role in inputting coastal morpho-hydrodynamic modeling data in coastal area management [15]. The important role of shallow water bathymetric information is directly proportional to the various methods developed to obtain increasingly precise accuracy.

Obtaining shallow water bathymetric information based on remote sensing or Satellite-Derived bathymetry is an alternative to the lack of data in areas that are difficult to reach by conventional bathymetric mapping methods such as single-beam sonar (SBS), multibeam sonar (MBS), because in general there are fundamental problems in surveys Conventional is efficient because it carries massive equipment and adequate ships, making it difficult to enter sensitive, remote and unfamiliar waters, and its scope of operations is limited [16].

Accuracy is still a "Pandora's box" that continues to haunt the results of SDB processing, and is an issue that continues to be studied in depth and reported on an ongoing basis [9], depending on variations in the quality of satellite imagery [17], the quality and content of aquatic suspensions [18], and mapping methods [19]. Two general approaches used to obtain shallow water depth via satellite include physics-based with the assumption of a radiation transfer model [17] and [20], and empirical algorithm-based developed by [21] and [22] combined with multiple regression and log spectral ratio regression [17]. Several recent investigations have shown good results in the accuracy of water depth estimation using machine learning (ML) approaches [23] with RMSE below 1 meter [8] and [24]. Previous research using an empirical approach on PlanetScope imagery still shows fluctuating accuracy with a range of below 1 meter [25], and between 2 – 3 meters [26]. On the Sentinel-2A image side, using an empirical approach, the accuracy is shown to be around 1 meter [27]. In this study, we tested the performance of Stumpf's (2003) empirical computational model for mapping shallow water bathymetry, with the complexity of bottom types of waters and coral reef ecosystems and involving two types of images with different resolutions, namely PlanetScope (spatial resolution: 3 meters) specifically on the Red Edge, Green I, Yellow, and Coastal Blue and Sentinel-2A channels (10 meter spatial resolution on visible channels). The entire series of processes in this research were carried out on a cloud-based computing platform: Google Earth Engine.

2. Study Area

This study was carried out in optically shallow waters in the Karimunjawa Islands region, namely one of the main islands - Kemujan (see Figure 1). This island is part of the Karimunjawa National Park, and has a number of local communities. Geomorphic classes that appear in the waters of this island include diverse coral reefs and variations in underwater topography [9].

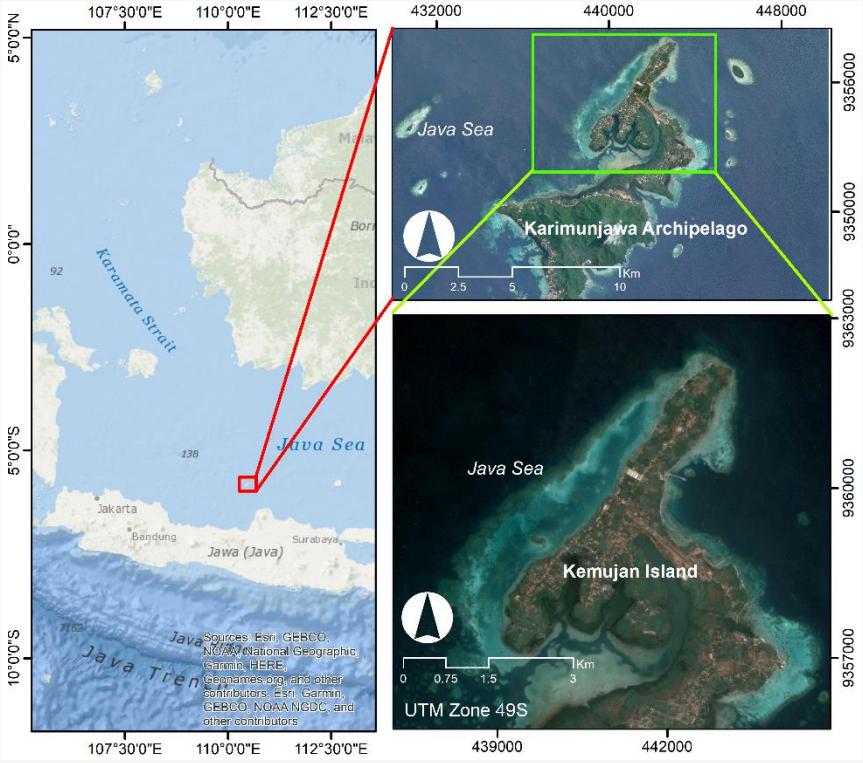

Figure 1: Kemujan island, Indonesia

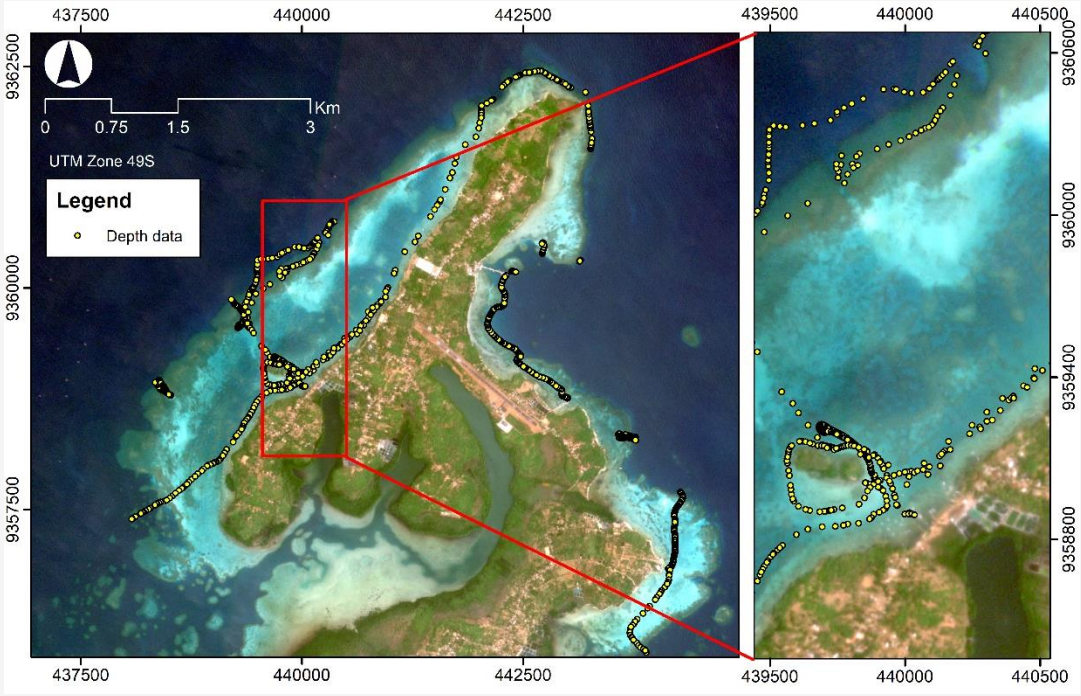

Figure 2: Depth data from in-situ sounding results used as

The Karimunjawa Islands have unique characteristics, where the commonly found geomorphology of benthic habitats are Reef Flat, Reef Cut, Fore Reef, Bank/Shelf, and Escarpment [28]. Flat reefs, shallow lagoons, reef backwards, peak reef, precursor, spur and stream, and patch reef in the shallow lake are found on the western side of the research area. Flat, cut, crest, front, spur, and stream on the east side. Because the change in reflectivity is dependent on both the base type's variation in reflection and the water column's energy retention, the variable base type is ideal for evaluating approaches in the field of research [9].

3. Methods

3.1 In-Situ Data Collection

Acquisition of actual depth of field data was measured in stages in 2021 [9], which was supplemented with measurement data from 2016 [29] and 2009 [30]. The distribution of depth samples from in-situ measurements can be seen in Figure 2. Depth data was taken conventionally using a ship equipped with a Garmin GPSMap 2108 single-beam echo sounder instrument. Even though the data was taken in different years, [9] stated that the study area is included in a national park area so that the bottom topography of the waters tends to be consistent from 2009 to 2021 because it has not experienced significant conversion, but corrections still need to be made. to the average sea level height. Field depth data is divided into modeling samples and verification samples to train and validation algorithms for evaluate mapping accuracy. It takes into account trunk characteristics and depth coverage to ensure a balanced representation of depth ranges and variations in the training and validation sets. There are at least 1733 data which are then divided randomly into 70% for training and 30% for validation. The distribution of depth points for training and validation is completely done automatically via GEE.

3.2 Imagery Data

The PlanetScope image used in this study is an image recorded on October 28 2023, with almost 0% cloud cover. The PlanetScope constellation consists of approximately 120 satellites. Every day, they will be able to produce satellite images of the Earth's surface with a spatial resolution of 3 m and a radiometric resolution of 12 bits [28]. In this study, we conducted performance trials on the new channels added by Planet, namely Red Edge, Green I, Yellow, and Coastal Blue (for more complete specifications, see Table 1). The data obtained has been carried out through automatic mosaic and composite processes by a system provided by Planet in *https://www.planet.com/*.

Tabel 1: PlanetScope imagery specification with four additional channels [31]

Band No.	Name	Wavelength (nm)
1	Coastal Blue	431 - 452
2	Blue	465 – 515
3	Green I	513 - 549
4	Green	547 – 583
5	Yellow	600 - 620
6	Red	650 – 680
7	Red Edge	697 – 713
8	NIR	845 – 885

The Sentinel-2A as a more general dataset image used was obtained directly from the Earthengine Catalog database with Surface Reflectance (SR) processing. The selected recording date is relatively close to the PlanetScope image recording dateSentinel-2A imagery has 12-bit radiometric quantization and thirteen spectral bands ranging from visible to shortwave infrared (SWIR). It employs four bands (red, green, blue, and near infrared) with a spatial resolution of 10 m, six 20 m bands, and three 60 m bands, including a high-penetration coastal aerosol band [17]. The selected Sentinel-2A image was filtered automatically using GEE, where the selected cloud cover was <10% and cloud masking was carried out automatically.

3.3 Cloud Processing Workflow

We use the cloud platform - Google Earth Engine (GEE) to carry out processing of the entire series of SDB acquisition activities. We filter non-aquatic features that have the potential to produce bias, such as clouds, waves and sunglints. Then we separate land from water using the NDWI (Normalized difference water index) formula as presented in Equation 1.

$$NDWI = \frac{\rho(Green) - \rho(NIR)}{\rho(Green) + \rho(NIR)}$$

Equation 1

Where *ρ(Green)* is reflectance of green band, and *ρ(NIR)* is reflectance of near infrard (NIR) band on multispectral imagery. By limiting the NDWI value to a certain threshold, the transformation results can be used as geometry to cut water areas. In the Sentinel-2 image the channels involved are blue and green, but in PlanetScope we tried various possibilities, namely Coastal Blue and Green I, Coastal Blue and Yellow, and Coastal Blue and Red edge channels. The channel is then applied to the equation developed by [22] using a band ratio so that the depth is independently expected to approach the albedo value of the bottom of the water. The equation is written in Equation 2.

$$z = m_1 \frac{(\ln(nR_w(\lambda_i))}{(\ln(nR_w(\lambda_j))} - m_0$$

Equation 2

Where *z* is model depth, λ is spectral bands, m_1 is a constant used to scale the ratio to depth, with *n* a fixed value for all locations and offset denoted as m_0 [22].

3.4 Accuracy Assessment

To assess the capabilities of the two images used (PlanetScope and Sentinel-2), we carried out accuracy calculations to evaluate the results of shallow water bathymetry maps. The total data used to calculate accuracy is 40% of the total data measured in the field. Accuracy testing uses two methods, R-squared (R^2) and Root Mean Square Error (RMSE) as presented in Equations 3 and 4 [32].

$$R^2 = 1 - \frac{\sum_i (h_i - h_i^{'})^2}{\sum_i (h_i - h_i^{''})^2}$$

Equation 3

$$RMSE = \sqrt{\frac{\sum_{i=1}^{n} \left(h_i - h_i^{'}\right)^2}{n}}$$

Equation 4

Where h is the reference depth, h_i' defined as the depth of the SDB results model, and $h_i^{''}$ is the average reference depth, and n is the amount of data [32]. Accuracy Assessment is carried out entirely within the Google Earth Engine platform, thereby reducing human intervention in the process.

4. Results and Discussion

4.1 Shallow Water Image

According to [33], shallow water, especially optically, is a water area that can be penetrated by sunlight until it reaches the bottom of the water effectively. The NDWI transformation results that were successfully obtained were then used to cut a specific study area in the optically shallow waters around the waters of Kemujan Island. Deep water and land areas will automatically be separated from shallow water. We use different thresholds on the two images to determine the threshold NDWI value used to cut the main image. The cropped image (see Figure 3) will be input for further processing from SDB. Visually it can be seen that the optical shallow water produced by Sentinel-2A leaves no residue as shown by the results of the PlanetScope imagery.

4.2 Bathymetry Results Distributions

We carried out systematic testing of new channels from Citra PlanetScope with a combination of Coastal Blue and Green I, Coastal Blue and Yellow, and Coastal Blue and Red edge channels. The channels used in Sentinel-2A imagery are relatively common, namely Blue and Green. The spatial distribution of depth produced by each combination does not show a similar pattern. However, the SDB computing results with the Coastal Blue/Green I and Coastal Blue/Red Edge combinations have a slightly similar pattern with relatively the same depth range, namely in the range -1 to -5.9. The depth distribution produced by SDB with Sentinel-2A image data input produces smoother visualization of the water bottom when compared to other channel combinations. The combination of the Coastal blue and yellow band produces a depth with an excessive value of -23.2 meters (see Figure 4).

We took cross section at two different locations on the West and East sides of Kemujan Island (see Figure 5). At the first transect location, the SDB results in the coastal blue and red edge (CBRE) combination band have a depth profile pattern that is similar to the coastal blue and green 1 (CBG1) combination band (see Figure 4, Blue and Orange lines). SDB results from the Sentinel 2 MSI image (combination of blue and green bands) on the first transect produce the deepest values at a distance of 300 – 400 m from the coastline. A similar pattern is also shown by the SDB results from the PlanetScope combination of coastal blue and yellow (CBY) imagery. Transect 1 is taken from the coastline to the optical deep waters boundary, where this boundary is generally characterized by an increase in base height in the reef crest area [33]. The shallow water area of the western part of Kemujan Island generally forms a valley, where according to observations [34] based on transects at relatively the same location it can be seen that the bathymetry near the coast tends to be gentle, which then becomes deeper to form a valley before finally rising to become shallower in the reef crest area. This pattern can also be identified in the multispectral image in Figure 3, where the central area of the transect tends to have a darker hue compared to the area near the coast and reef crest (dark means it tends to be deeper). This bathymetric pattern can be well represented by SDB results using Sentinel 2 MSI and PlanetScope imagery with a combination of coastal blue and yellow bands (see Figure 6). The other two combinations were not able to represent the bathymetric pattern properly.

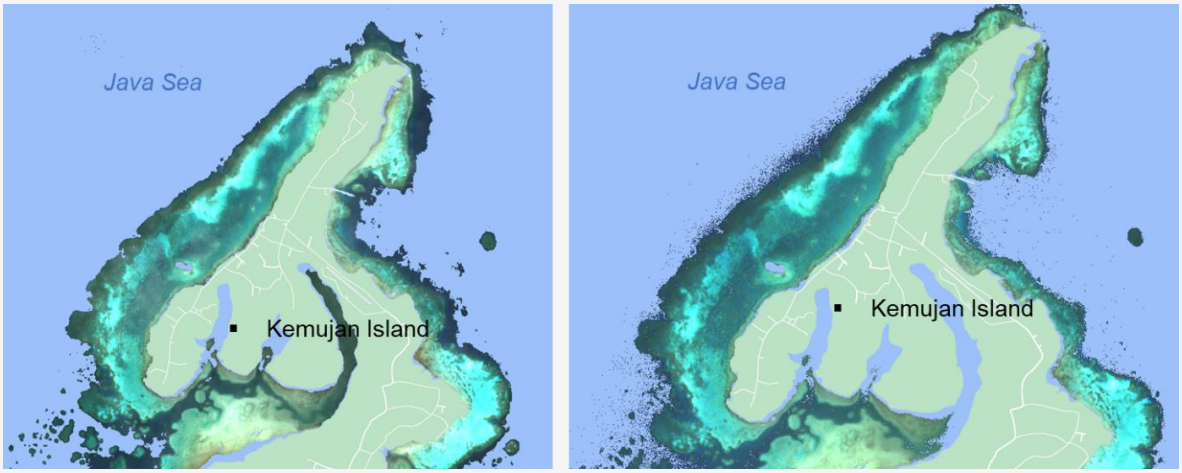

Figure 3: Areas of shallow water that have been separated from land and deep water from Sentinel-2A (Left) and PlanetScope (Right) imagery

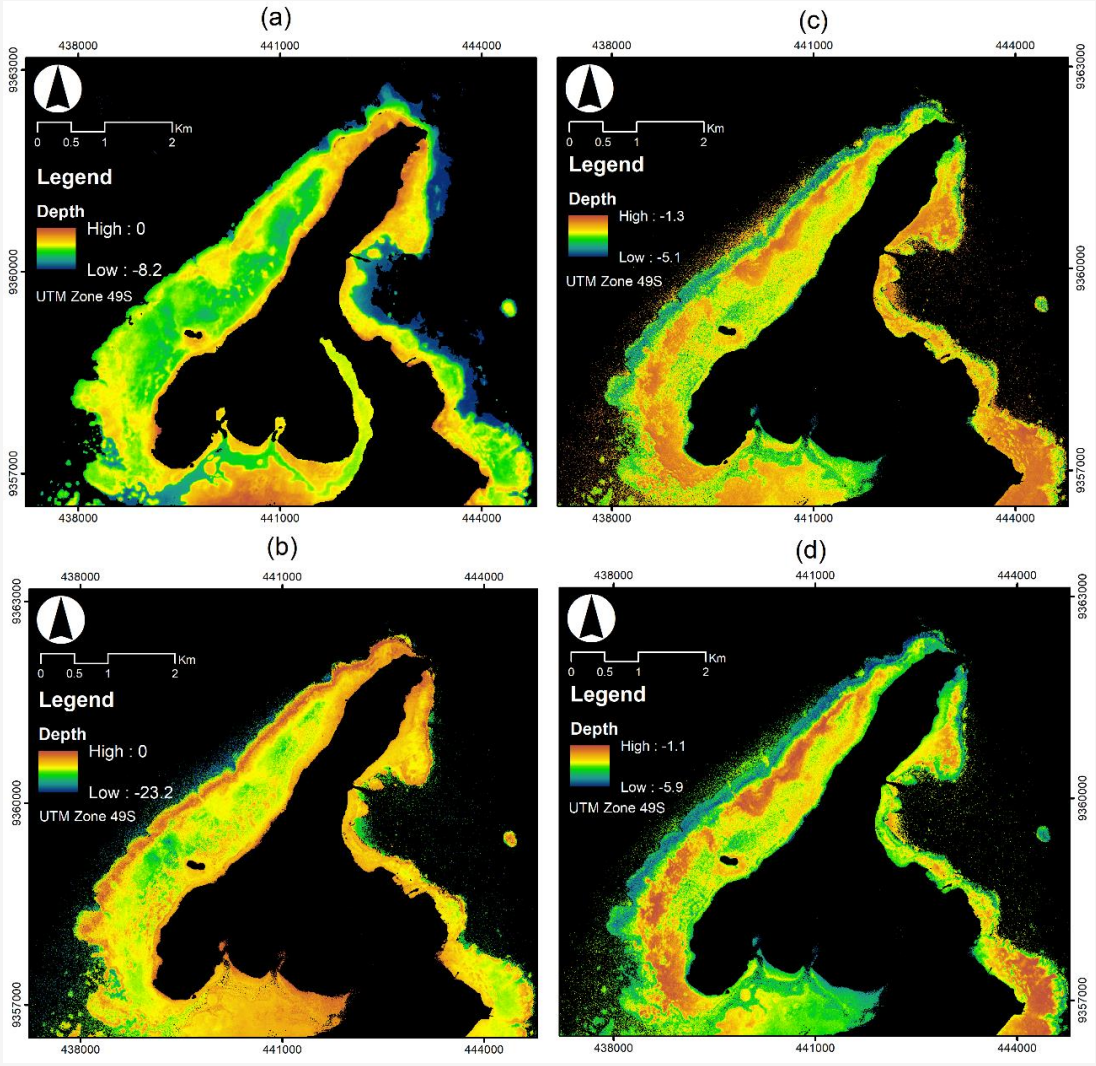

Figure 4: Shallow water bathymetry results from SDB computing using the empirical method developed by [22] using combination band of: (a) Sentinel 2A MSI, (b) Planetscope coastal blue/yellow, (c) coastal blue and green 1, and (d) coastal blue and red edge

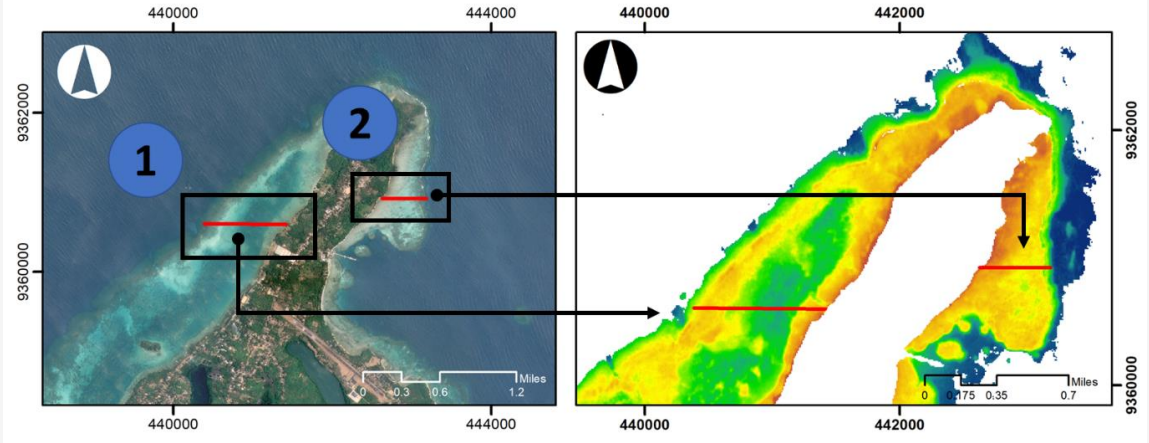

Figure 5: Location of cross-sectional sampling at transect 1 in the western part and transect 2 in the eastern part of Kemujan Island

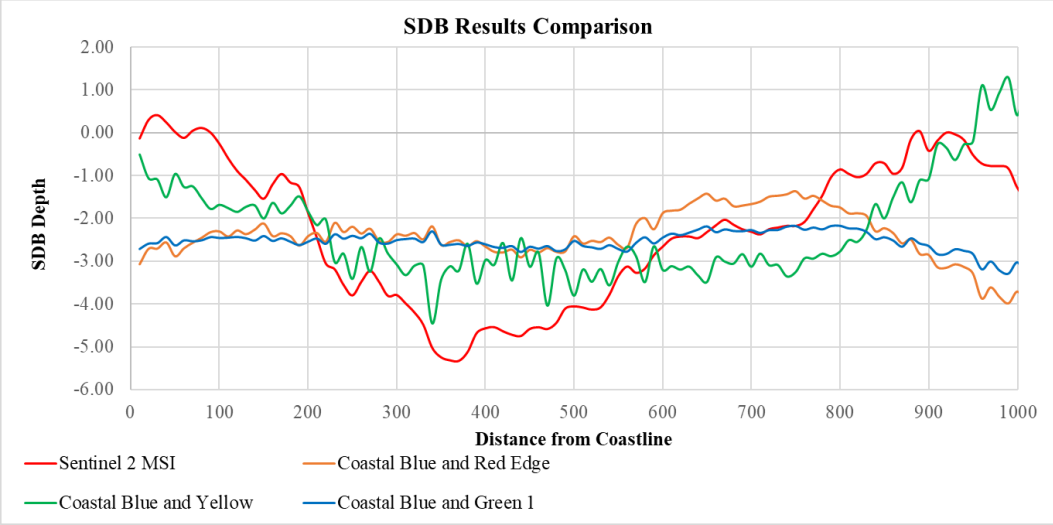

Figure 6: Vertical profile on transect 1 on four SDB results based on the band combination used

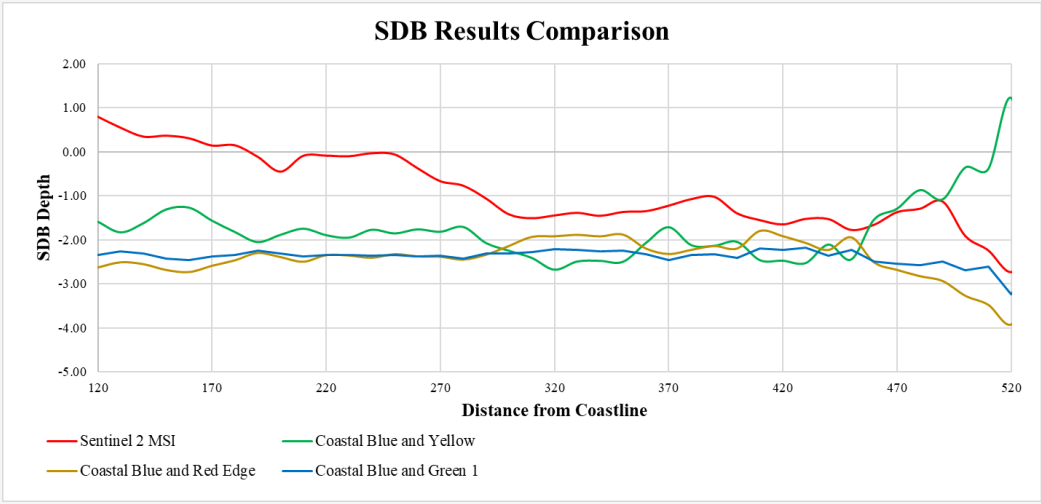

Figure 7: Vertical profile on transect 2 on four SDB results based on the band combination used

In transect 2 (eastern part of Kemujan Island waters) the resulting bathymetric pattern tends to be uniform, but a different pattern is shown by the SDB results from the planetscope image with a combination of coastal blue and yellow at the end of the transect. The results of the SDB vertical bathymetric profile in the four scenarios show that there is no significant change in depth, and the water area of the eastern part of Kemujan Island which is represented by transect 2 tends to be sloping and constant (see Figure 7). The vertical profile is able to describe the similarity of the patterns of each SDB model produced in a systematic measurement.

4.3 RMSE and R^2 Comparison

In general, a summary of the accuracy test results can be seen in Table 2 for SDB results from computing Sentinel-2A and PlanetScope images with various combinations. Based on the results of accuracy tests carried out on all channel combinations, the best RMSE value was obtained and the channel was able to best represent the depth variations of all channels.

Based on the results of the channel combination accuracy test on Sentinel-2A imagery, it produces the best accuracy when compared with PlanetScope imagery on all channel combinations. The combination of channels in Sentinel-2A imagery is also able to represent depth variations in the study area reaching 70%. However, the combination of PlanetScope images with RMSE values that can still be studied further is the combined SDB results from the Coastal Blue/Yellow channel with an error accuracy of around 1.5 meters and still able to represent depth variations of up to 47%.

Table 2: Accuracy test results for each channel combination used

No	Band Combination	RMSE	R^2
1	Sentinel-2A (Blue/Green)	0.8	0.700
2	PlanetScope (Coastal Blue/Green I)	1.9	0.008
3	PlanetScope (Coastal Blue/Yellow)	1.5	0.470
4	PlanetScope (Coastal Blue/Red Edge)	1.9	0.070

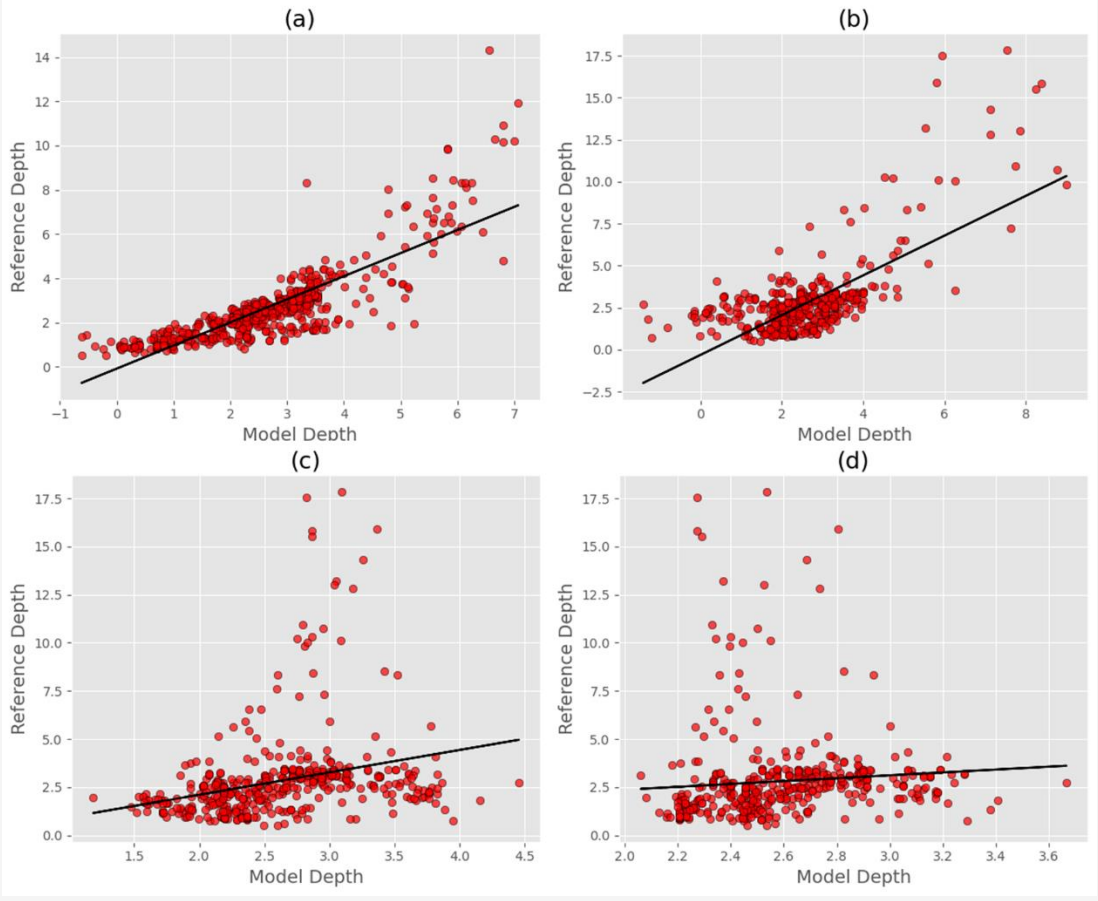

Figure 8: 1:1 plot of bathymetric data from SDB results (model) with depth references using the Stumpf algorithm applied to a combination of: (a) Sentinel 2 MSI, (b) CBY, (c) CBRE, and (d) CBG1 bands

Figure 8 presents a 1:1 comparison plot, where the results on Sentinel 2 MSI are the most accurate of the four SDB results. The SDB model that uses a combination of bands on Sentinel 2 MSI has high accuracy at a depth of 1 – 4 m. Accuracy begins to decrease when entering a depth of 4 – 7 m. In the new band planetscope image, the best combination that can be obtained is coastal blue and yellow. The best accuracy in planetscope images combining the coastal blue and yellow bands is at a depth of 2 – 4 m.

5. Conclusion

The use of cloud-based computing platforms such as Google Earth Engine enables effective remote sensing image processing to obtain water depth information. This research conducts performance tests on new bands published by planetscope imagery, namely coastal blue and yellow, coastal blue and red edge, and coastal blue and green 1. Sentinel 2A MSI satellite imagery is used as a more stable comparison and is commonly used in bathymetric modeling via SDB.

The empirical method uses the Stumpf algorithm approach applied to Sentinel-2A imagery and new channels in PlanetScope. In general, the SDB model obtained through Sentinel-2A MSI imagery provides satisfactory results in terms of accuracy (RMSE: 0.8) and the ability to represent the water model up to 70%. Promising results can be seen in the new band of planetscope imagery with a combination of CBY which is able to represent almost 50% of the bathymetry model with an accuracy of RMSE: 1.5 m. Through the SDB vertical profile, it can be seen that the pattern shown by the CBY band combination is similar to the SDB model pattern from the sentinel 2A MSI image which has good accuracy. Other new band combinations cannot provide representative SDB model results. This research found that the new band in the planetscope ideal, especially CBY, has the potential to be used in mapping shallow water bathymetry via SDB with promising results. Further research needs to be carried out to improve the accuracy and capability of the model to represent water depth.

Acknowledgement

The author thanks Universitas Gadjah Mada, where this research was funded by Gadjah Mada University through the Final Project Recognition Grant Universitas Gadjah Mada Number 5075/UN1.P.II /Dit-Lit/PT.01.01/2023 or RTA Program Universitas Gadjah Mada with the Grant Number 5075/UN 1.P.II/Dit-Lit/PT.01.01/2023, and PlanetScope to provide the imagery data.

References

[1] Vizzari, M., (2022). Object-Based Land Cover Classification in Google Earth Engine. *Remote Sensing.* Vol. 14. 1–19. https://doi.org/10.3390/ rs14112628.

[2] Tarca, G., Hoelzle, M. and Guglielmin, M., (2022). Using PlanetScope Images to Investigate the Evolution of Small Glaciers in the Alps. *Remote Sensing Applications: Society and Environment*, Vol. 32. https://doi.org/ 10.1016/j.rsase.2023.101013.

[3] Acharki. S., (2022). PlanetScope Contributions Compared to Sentinel-2, and Landsat-8 for LULC Mapping, *Remote Sensing Applications: Society and Environment*, Vol. 27. https://doi. org/10.1016/j.rsase.2022.100774.

[4] Paulino, R. S., Martins, V. S., Novo, E. M. L. M., Maciel, D. A., Correia-Lima, D. L., Barbosa, C. C. F., Bonnet, M. P. and Uhde, A., (2023). A Framework Based on Spectral Similarity to Estimate Hydrological Connectivity in Juruá River Floodplain Lakes Using 3-m PlanetScope Data. *Journal of Hydrology*, Vol. 625. https://doi.org/10.1016/j.jhydrol.2023.130 156.

[5] Schaeffer, B. A., Whitman, P., Conmy, R., Salls, W., Coffer, M., Graybill, D., and Lebrasse, M. C. (2022) Potential for Commercial PlanetScope Satellites in Oil Response Monitoring, *Marine Pollution Bulletin.* Vol. 183. https://doi.org/10.1016/j.m arpolbul.2022.114077.

[6] Evagorou, E., Argyriou, A., Papadopoulos, N., Mettas, C., Alexandrakis, G. and Hadjimitsis, D., (2022). Evaluation of Satellite-Derived Bathymetry from High and Medium-Resolution Sensors Using Empirical Methods, *Remote Sensing*, Vol. 14(3). https://doi.org/10.3390/ rs140 30772.

[7] Li, J., Knapp, D. E., Schill, S. R., Roelfsema, C., Phinn, S., Silman, M., Mascaro, J. and Asner, G. P., (2019). Adaptive Bathymetry Estimation for Shallow Coastal Waters Using Planet Dove Satellites, *Remote Sensing of Environment.* Vol. 232. https://doi.org/10.1016/ j. rse.2019.111302.

[8] Sagawa, T., Yamashita, Y., Okumura, T. and Yamanokuchi, T., (2019) Satellite Derived Bathymetry Using Machine Learning and Multi-Temporal Satellite Images, *Remote Sensing*, Vol. 11. https://doi.org/10.3390/rs111 01155.

[9] Wicaksono, P., Djody Harahap, S. and Hendriana, R., (2024) Satellite-Derived Bathymetry from WorldView-2 Based on Linear and Machine Learning Regression in the Optically Complex Shallow Water of the Coral Reef Ecosystem of Kemujan Island. *Remote Sensing Applications: Society and Environment*, Vol. 33. https://doi.org/10.1016/ j.rsa se.2023.101085.

[10] Zhong, J., Sun, J., Lai, Z. and Song, Y. (2022). Nearshore Bathymetry from ICESat-2 LiDAR and Sentinel-2 Imagery Datasets Using Deep Learning Approach, *Remote Sensing*, Vol. 14(17). https://doi.org/10.3390/rs14174229.

[11] Al Najar, M., Thoumyre, G., Bergsma, E. W. J., Almar, R., Benshila, R. and Wilson, D. G., (2023) Satellite Derived Bathymetry Using Deep Learning. *Machine Learning*, Vol. 112(4). 1107–1130, https://doi.org/10.1007/s1099402 1-05977-w.

[12] Wedding, L. M., Friedlander, A. M., McGranaghan, M., Yost, R. S. and Monaco, M. E., (2008). Using Bathymetric Lidar to Define Nearshore Benthic Habitat Complexity: Implications for Management of Reef Fish Assemblages in Hawaii. *Remote Sensing of Environment*, Vol. 112(11). https://doi.org/10.1016/j.rse.2008.01.025.

[13] Janowski, L., Trzcinska, K., Tegowski, J., Kruss, A., Rucinska-Zjadacz, M. and Pocwiardowski, P., (2018). Nearshore Benthic Habitat Mapping Based on Multi-Frequency, Multibeam Echosounder Data Using a Combined Object-Based Approach: A Case Study from the Rowy Site in the Southern Baltic Sea. *Remote Sensing*, Vol. 10(12). https://doi/10.3390/rs10121983.

[14] Chénier, R., Faucher, M. A. and Ahola, R., (2018). Satellite-derived Bathymetry for Improving Canadian Hydrographic Service Charts. *ISPRS International Journal of Geo-Information*, Vol. 7(8). https://doi.org/10.3390/ijgi 7080306.

[15] Lu, X., Hu, Y., Omar, A., Yang, Y., Vaughan, M., Rodier, S., Garnier, A., Ryan, R., Getzewich, B. and Trepte, C., (2022). Nearshore Bathymetry and Seafloor Property Studies from Space Lidars: CALIPSO and ICESat-2. *Optics Express*, Vol. 30(20). https://doi.org/10.1364/oe.471444.

[16] Wang, J., Tang, Y., Jin, S., Bian, G., Zhao, X. and Peng, C., (2023). A Method for Multi-Beam Bathymetric Surveys in Unfamiliar Waters Based on the AUV Constant-Depth Mode. *Journal of Marine Science and Engineering*, Vol. 11(7). https://doi.org/10.3390/jmse11071466.

[17] Mudiyanselage, S. S. J. D., Abd-Elrahman, A., Wilkinson, B. and Lecours, V., (2022). Satellite-derived Bathymetry Using Machine Learning and Optimal Sentinel-2 Imagery in South-West Florida Coastal Waters. *GIScience Remote Sensing*, Vol. 59(1). 1143–1158. https://doi.org/10.1080/15481603.2022.2100597.

[18] Ashphaq, M., Srivastava, P. K. and Mitra, D., (2023). Preliminary Examination of Influence of Chlorophyll, Total Suspended Material, and Turbidity on Satellite Derived-Bathymetry Estimation in Coastal Turbid Water. *Regional Study of Marine Science.* Vol. 62. https://doi.org/10.1016/j.rsma.2023.102920.

[19] Chu, S., Cheng, L., Cheng, J., Zhang, X. and Liu, J., (2023). Comparison of Six Empirical Methods for Multispectral Satellite-derived Bathymetry, *Marine Geodesy*, Vol. 46(2). 149–174. https://doi.org/10.1080/01490419.2022.2132327.

[20] Brando, V. E., Anstee, J. M., Wettle, M., Dekker, A. G., Phinn, S. R. and Roelfsema, C., (2009). A Physics Based Retrieval and Quality Assessment of Bathymetry from Suboptimal Hyperspectral Data. *Remote Sensing of Environment*, Vol. 113(4). https://doi.org/10.1016 /j.rse.2008.12.003.

[21] Lyzenga, D. R., (1978). Passive Remote Sensing Techniques for Mapping Water Depth and Bottom Features, *Applied Optics*, Vol. 17(3). https://doi.org/10.1364/ao.17.000379.

[22] Stumpf, R. P., Holderied, K. and Sinclair, M., (2003). Determination of Water Depth with High-Resolution Satellite Imagery Over Variable Bottom Types. *Limnology Oceanography*, Vol. 48(1). https://doi.org/10.4319/lo.2003.48.1_part_2.0547.

[23] Tonion, F., Pirotti, F., Faina, G. and Paltrinieri, D., (2020). A Machine Learning Approach to Multispectral satellite Derived Bathymetry. *ISPRS Annals of the Photogrammetry, Remote Sensing and Spatial Information Sciences*. Vol. 5(3). https://doi:10.5194/isprs-Annals-V-3-2020-565-2020.

[24] Manessa, M. D. M., Kanno, A., Sekine, M., Haidar, M., Yamamoto, K., Imai, T. and Higuchi, T., (2016). Satellite-Derived Bathymetry Using Random Forest Algorithm and Worldview-2 Imagery. *Geoplanning: Journal of Geomatics and Planning*, Vol. 3(2). https://doi:10.14710/geoplanning.3.2.117-126.

[25] Wulandari, S. A. and Wicaksono, P., (2021). Bathymetry Mapping Using PlanetScope Imagery on Kemujan Island, Karimunjawa, Indonesia. *IOP Conf. Ser. Earth Environ. Sci.*, Vol. 686(1), https://doi:10.1088/1755-1315/686/1/012032.

[26] Sesama, A. S., Setiawan, K. T. and Julzarika, A., (2021). Bathymetric Extraction Using Planetscope Imagery (Case Study: Kemujan Island, Central Java), *International Journal of Remote Sensing and Earth Sciences (IJReSES)*, Vol. 17(2). https://doi:10.30536/j.ijreses.2020.v17.a3445.

[27] Rahman, A., Siregar, V. P. and Panjaitan, P. J., (2020). Estimasi Kedalaman Perairan Dangkal Menggunakan Citra Satelit Multispektral Sentinel-2a. *Segara*, Vol. 8(2), 151 - 162. http://dx.doi.org/10.15578/segara.v16i3.8562.

[28] Wicaksono, P. and Lazuardi, W., (2018). Assessment of PlanetScope Images for Benthic Habitat and Seagrass Species Mapping in a Complex Optically Shallow Water Environment. *International Journal of Remote Sensing*, Vol. 39(17). https://doi.org/10.1080/01431161.2018.1506951.

[29] Rahman, W. and Wicaksono, P., (2019). Aplikasi Citra WorldView-2 untuk Pemetaan Batimetri di Pulau Kemujan Taman Nasional Karimunjawa. *Jurnal Penginderaan Jauh Indonesia*, Vol. 1(1), http://jurnal.mapin.or.id/index.php/jpji/issue/view/1.

[30] Wicaksono, P., (2010). I*ntegrated Model of Water Column Correction Technique for Improving Satellite-Based Benthic Habitat Mapping, A Case Study on Part of Karimunjawa Islands, Indonesia*. Master Thesis, Universitas Gadjah Mada, Indonesia.

[31] ESA, (2024). PlanetScope Instruments. Available at: https://earth.esa.int/eogateway/missions/planetscope [Accessed January 12, 2024].

[32] Manessa, M. D. M., Kanno, A., Sekine, M., Haidar, M., Yamamoto, K., Imai, T. and Higuchi, T., (2016). Satellite-Derived Bathymetry Using Random Forest Algorithm and Worldview-2 Imagery. *Geoplanning: Journal of Geomatics and Planning*, Vol. 3(2). https://doi.org/10.14710/geoplanning.3.2.117-126.

[33] Solihuddin, T., Nasution, D. A., Salim, H. L. and Mustikasari, E., (2020). Reef Geomorphology and Associated Habitats of Karimunjawa Islands, Indonesia: a Spatial Approach to Improve Coastal and Small Islands Management. *Jurnal Segara*, Vol. 16(2). https://doi.org/10.15578/segara.v16i2.8385.

[34] Wicaksono, P., (2016). Improving the Accuracy of Multispectral-Based Benthic Habitats Mapping Using Image Rotations: The application of Principle Component Analysis and Independent Component Analysis. *European Journal of Remote Sensing*, Vol 49. https://doi.org/10.5721/EuJRS20164924.